Aerosol and Air Quality Research, 17: 896–907, 2017

ISSN: 1680-8584 print / 2071-1409 online
doi: 10.4209/aaqr.2016.07.0321

Characterization of Chemical Composition in $PM_{2.5}$ in Beijing before, during, and after a Large-Scale International Event

Xiaowen Yang[1], Shuiyuan Cheng[1,2*], Jianbing Li[3], Jianlei Lang[1], Gang Wang[1]**

[1] *Key Laboratory of Beijing on Regional Air Pollution Control, Beijing University of Technology, Beijing 100124, China*
[2] *Collaborative Innovation Center of Beijing City Traffic, Beijing University of Technology, Beijing 100124, China*
[3] *Environmental Engineering Program, University of Northern British Columbia, Prince George, British Columbia V2N 4Z9, Canada*

ABSTRACT

To commemorate the 70th anniversary of the victory of the Chinese people's Anti-Japanese War and the World Anti-Fascist War, an international parade was held in Beijing in September 2015. In order to ensure satisfactory air quality during this event, a phased emission control measures were taken in Beijing and its surrounding provinces. The 24-h $PM_{2.5}$ samples were collected in Beijing from August 1 to September 15, 2015 covering the period before, during and after this large-scale event. The observed $PM_{2.5}$ data, meteorological data, emission reduction measures, and air mass trajectory simulation results were systematically analyzed to understand the pollution characteristics and chemical compositions of $PM_{2.5}$ in Beijing. The results indicated that $PM_{2.5}$ concentration during the two emission control phases was reduced by 61.7% comparing to the non-control period, but the regional transport of pollutants and meteorological conditions had a more prominent impact on $PM_{2.5}$ than emission reduction during phase 2. The secondary water-soluble ions including SO_4^{2-}, NO_3^-, and NH_4^+ were found as the main ions present in $PM_{2.5}$. During the entire emission control period, organic carbon (OC) and elemental carbon (EC) mass concentrations were decreased by 53.1% and 57.9%. A $PM_{2.5}$ mass balance was analyzed, and it was found that the organic matter accounted for 29.3, 37.6 and 28.5% of the $PM_{2.5}$ mass before, during and after the emission control, while the contribution of mobile sources to $PM_{2.5}$ was relatively outstanding after a series of emission control measures.

Keywords: Air mass trajectory; Chemical composition; Emission control; Water-soluble ion; $PM_{2.5}$.

INTRODUCTION

Northern China has experienced significant economic growth over the past 30 years as a result of rapid industrialization and urbanization. However, such economic prosperity has also put tremendous pressure on the local and regional environment (Ji *et al.*, 2014). Especially, the frequently occurred haze pollution problems in this region have attracted widespread attention in recent years (Li and Han, 2015; Huang *et al.*, 2015). For example, northern China experienced severe haze episodes with long duration which affected unusually sizeable areas in January 2013, October 2014 and December 2015, respectively (Wang *et al.*, 2014a; Tang *et al.*, 2015). Many studies have shown that $PM_{2.5}$ is a main cause of haze problem, which can have adverse effects on visibility, human health, and even global climate (Song *et al.*, 2012; Fann and Risley, 2013; Wang *et al.*, 2014b). The investigation of $PM_{2.5}$ characteristics and its formation mechanism is thus of critical importance.

Beijing, the capital city of China, is one of the largest megacities in the world. It has more than 21.5 million residents and 5.6 million vehicles in 2014 (BMBS, 2015). Located in northern China, its main topography is plain, but it is surrounded by the Taihang and Yanshan mountains at approximately 1000–1500 m above sea level in the west, north, and northeast, respectively (Chen *et al.*, 2015). This special terrain environment is beneficial to trap air pollutants. Previous studies indicated that air pollution in Beijing was affected not only by its local emission, but by pollutant transport from its surrounding provinces (Tao *et al.*, 2013). Under the stable weather condition, high density air pollution can be easily formed. As the center of politics, culture, international exchange and technological innovation of China, Beijing hosted various large-scale international events, such as the 2008 Olympic Games and the 2014 Asia-Pacific

* Corresponding author.
Tel.: +86 10 67391656; Fax: +86 10 67391983
E-mail address: chengsy@bjut.edu.cn
** Corresponding author.
Tel.: +1 250 9606397; Fax: +1 250 9605845
E-mail address: Jianbing.Li@unbc.ca

Economic Cooperation (APEC) Summit. In order to ensure satisfactory air quality during such events, the Chinese government has implemented stringent air pollution control measures (e.g., shutting down factories, restriction of vehicles on road) in Beijing and its surrounding areas (Meng *et al.*, 2015). These measures have provided a valuable opportunity to investigate the characteristics of regional air pollution under the effect of emission reduction. Some studies have been reported to examine the properties and formation mechanism of $PM_{2.5}$ in Beijing. For example, Okuda *et al.* (2011) investigated the difference in the concentrations of air pollutants between the period of the 2008 Olympic Games and the same periods during the prior three years, and they observed that many ions in $PM_{2.5}$ decreased during the Game period, but NO_3^- increased significantly. Schleicher *et al.* (2012) analyzed the elemental characteristics of $PM_{2.5}$ before, during, and after the period of the 2008 Olympic Games, and they found that elements from anthropogenic sources were reduced more efficiently during the Olympic Games than those from geological sources. Gao *et al.* (2013) reported that the concentrations of SO_4^{2-}, NO_3^-, and NH_4^+ in $PM_{2.5}$ were closely related to meteorological conditions, primary emissions, and regional transport, and the high pollution observed after the full-scale emission control was attributed to regional transport from the south of Beijing. Xu *et al.* (2015) examined the impacts of emission controls on aerosol composition, size distributions, and oxidation properties, and their results indicated that both highly oxidized secondary organic aerosol (SOA) and secondary inorganic aerosol decreased during the 2014 APEC Summit. Based on observation data, analysis of emission reduction measures, and air quality simulations, Wen *et al.* (2016) investigated the $PM_{2.5}$ chemical composition change and the relationship between emissions and air pollutant concentrations during the 2014 APEC Summit, and they found that total $PM_{2.5}$ concentrations were reduced by 54% when compared to non-emission control period.

To commemorate the 70th anniversary of the victory of the Chinese People's Anti-Japanese War and the World Anti-fascist War, a large-scale international parade was held in Beijing on September 3, 2015. In order to improve the air quality during the parade, the government of Beijing cooperated with the governments of its surrounding regions including Hebei province, Tianjin city, Shanxi province, Shandong province, Inner Mongolia Autonomous Region, and Henan province (Fig. 1). A series of emission reduction measures were gradually implemented before and during this event, such as reducing the number of vehicles in operation by about 50%, shutting down factories, closing construction activities, and enhancing the cleanliness of urban roads. Different from previous emission reduction activities for large-scale events, a phased emission reduction program was adopted, including phase 1 from August 20 to 27, 2015 with emission reduction only in Beijing, and phase 2 from August 28 to September 4, 2015 with emission reduction both in Beijing and its surrounding provinces. Such phased emission control measures may result in different pollution characteristics of $PM_{2.5}$. As a result, it is of importance to study the chemical components of $PM_{2.5}$ during this special event for better understanding the pollution sources and formation mechanism in Beijing. The objective of this study is then to reveal the impact of the phased emission reduction on $PM_{2.5}$ pollution characteristics. The $PM_{2.5}$ samples were collected in Beijing from August 1 to September 15, 2015. The observed $PM_{2.5}$ and meteorological data as well as the emission reduction measures were systematically analyzed. The obtained results would help understand the formation and development of $PM_{2.5}$ pollution and thus provide scientific basis for air pollution control in Beijing.

METHODS

Emission Reduction Measures

Beijing and its surrounding provinces had taken a series of emission reduction measures (Fig. 1). More than 111

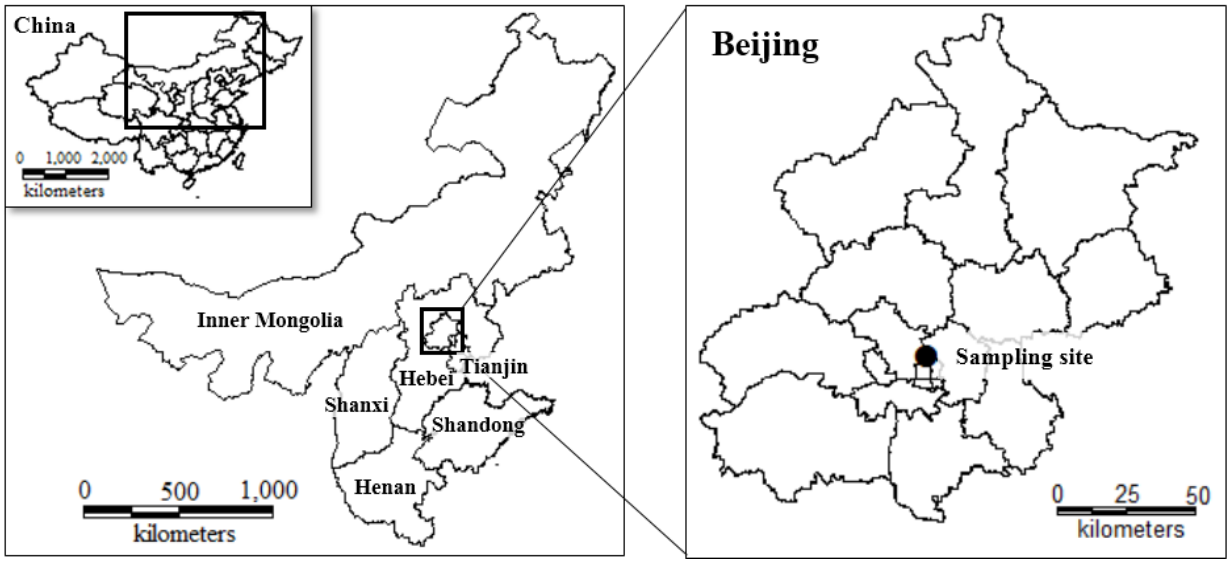

Fig. 1. Study area and sampling site location.

businesses with high emissions in Beijing were required to stop or limit their production from August 20 to September 4, 2015. Meantime, the odd-even rule was implemented in Beijing to restrict traffic emissions. Vehicles with license plates ending in odd number were banned from roads on even-numbered days, and those with plates ending in even number were banned from roads on odd-numbered days. In addition, 80% of government vehicles were prohibited on roads. During this emission control period, all construction activities were stopped. Trucks transporting mud and stone as well as heavy-emission vehicles were prohibited from roads in Beijing. Moreover, the road sweeping in Beijing was enhanced. Through a series of these measures, the emission reductions were 36.5% for SO_2, 49.9% for NO_x, 50.3% for PM_{10}, 49.0% for $PM_{2.5}$ and 32.4% for VOCs in Beijing (BMEPB, 2015). Furthermore, major provinces around Beijing had also taken a series of measures to reduce emissions from August 28 to September 4, 2015, and their emission reductions were over 30%. More than ten thousand enterprises were closed or ordered to limit production, and about 9000 construction sites were shut down during the emission control period in Beijing and its surrounding provinces (BMEPB, 2015). Table 1 summarizes the emission reductions and reduction ratio in Beijing.

Sample Collection

$PM_{2.5}$ was sampled during the period from August 1 to September 15, 2015 (Fig. 1). A total of 41 daily samples were collected, and there were no samples for 5 days taken due to rain and equipment failure. The samples were collected on the roof (35 m above ground) of a building in Beijing Normal University (39°57′N, 116°21′E), a site having mixed residential and traffic sources, but without major industrial sources. The sampling site was about 6.5 km away from the northwest of the city center (Tiananmen Square), and it could fairly represent the air quality in Beijing. The sampling time was from 9:00 a.m. to 9:00 a.m. of the next day. When faced with exceptional circumstances (rainy day and equipment failure), the temporary adjustment of sampling time was made. For the collection of $PM_{2.5}$ samples, a medium volume sampler (URG-3000ABC, USA) with a flow-rate of 8.35 L min^{-1} was used. Teflon filters (47 mm, Whatman, UK) and quartz filters (47 mm, Whatman, UK) were used as impaction substrates on alternate days. The Teflon samples were used for the analysis of PM mass, elements and inorganic ions, while the quartz samples were used for the analysis of carbonaceous species (Wen *et al.*, 2016). All of the samples were stored in a fridge at < 4°C before analysis.

Chemical Analysis

For analyzing PM mass concentrations, the Teflon filter were weighed before and after each sampling event using a microbalance (Sartorius-Denver TB-215D, accuracy, 0.01 mg) after stabilizing under constant temperature (20 ± 5°C) and humidity (40 ± 2%) for over 48h. For analyzing the concentrations of water-soluble ions, half of each Teflon filter sample was extracted ultrasonically by 10 mL of deionized water (with resistivity of 18.25 MΩ cm^{-1}). After passing through microporous membranes (pore size, 0.45 μm; diameter, 25 mm), the filtrates were determined for pH with a pH meter. The concentrations of six anions (F^-, Cl^-, NO_2^-, NO_3^-, PO_4^{3-}, SO_4^{2}) and five cations (Na^+, K^+, Ca^{2+}, Mg^{2+}, NH_4^+) were analyzed by Ion Chromatography (861 Advanced Compact IC, Metrohm) (Wang *et al.*, 2005).

For analyzing the concentrations of elements, half of each Teflon filter sample was digested at 170°C for 4 h in a high-pressure Teflon digestion vessel with 3 mL of concentrated HNO_3, 1 mL of concentrated $HClO_4$, and 1 mL of concentrated HF. After cooling, the solutions were dried and treated with 1 mL of concentrated HNO_3, and then diluted to 10 mL with deionized water. A total of 23 elements (Na, Mg, Al, S, Ca, Sc, Ti, V, Cr, Mn, Fe, Co, Ni, Cu, Zn, As, Se, Sr, Cd, Sb, Ce, Eu, and Pb) were determined for their concentrations by inductively coupled plasma mass spectrometry (ICP-MS, Agilent 7500A) (Fu *et al.*, 2008).

The thermal optical reflectance carbon analysis method for element carbon (EC) and organic carbon (OC) content was performed following the IMPROVE protocol (Chow *et al.*, 2004). The quartz filter sample was heated stepwise in pure He gas (no oxygen) at temperatures of 120°C (OC1), 250°C (OC2), 450°C (OC3), and 550°C (OC4), respectively, transforming the particulate carbon into CO_2. The filter was then heated in an environment of He with 2% oxygen, at temperatures of 550°C (EC1), 700°C (EC2), and 800°C (EC3), by which temperature the EC of the samples was released. OC in the carbonization process would form the pyrolyzed organic carbon (OP). The OC was defined by OC1 + OC2 + OC3 + OC4 + OP, while the EC was defined by EC1 + EC2 + EC3 – OP (Zhang *et al.*, 2015).

Methodological blank values were determined and subtracted from analytical results of the samples. All the analysis procedures were subject to strict quality control to avoid any possible contamination.

Meteorological Data

Meteorological parameters including wind speed, wind direction, ground temperature, relative humidity, visibility, and precipitation amount were obtained from the "Weather Underground" website (http://www.wunderground.com). Data obtained from this website were supplied by Beijing weather station which is located in Beijing Capital International Airport (40°04′N, 116°35′E), about 25 km apart from the northeast of the city center. All of the meteorological data were arranged to half-hour interval according to the $PM_{2.5}$ sampling time (9:00 am to 9:00 am next day). In addition, morning temperature profile was

Table 1. Emission reduction and reduction ratio during the emission control period in Beijing.

	SO_2	NO_x	PM_{10}	$PM_{2.5}$	VOCs
Emission reduction (t)	286.3	3655.5	5333.5	1276.2	2907.5
Reduction ratio (%)	36.5	49.9	50.3	49	32.4

drawn from aircraft meteorological data relay (AMDAR) at Beijing Capital International Airport. Using the morning temperature profile and the daily maximum ground temperature, the daily maximum mixing layer height was calculated by dry adiabatic method (Cheng *et al.*, 2002).

Air Mass Trajectory Analysis

In this study, air mass trajectory analysis was used to examine the impact of pollutant regional transport on pollution characteristics in Beijing. The 24-h back trajectories were calculated for each hour at 100 m height using the Hybrid Single-Particle Lagrangian Integrated Trajectory (HYSPLIT, NOAA) 4 model (Draxler and Hess, 1997). The trajectories were grouped into three clusters during phase 1 of emission reduction and five clusters during phase 2 using the algorithm of cluster analysis. The clustering of trajectories could minimize the inter-cluster differences among trajectories while maximizing the inter-cluster difference, and it has been widely used in many studies (Chen *et al.*, 2015; Li *et al.*, 2015).

RESULTS AND DISCUSSION

General Characteristics of $PM_{2.5}$

Fig. 2 shows the time series of $PM_{2.5}$ mass concentrations and major meteorological parameters during the entire study period. The daily $PM_{2.5}$ concentrations varied significantly from 10.3 to 122.6 μg m^{-3} and averaged at 49.6 ± 31.0 μg m^{-3}. As indicated in Fig. 2, the concentration of $PM_{2.5}$ in Beijing was affected by wind direction and wind speed. The concentration of $PM_{2.5}$ was much higher when the predominant wind direction was south. However, when the wind direction changed from the south to the north, the concentration of $PM_{2.5}$ rapidly decreased. Haze episodes with such cycle driven by meteorological conditions have also been observed many times in Beijing (Sun *et al.*, 2014; Chen *et al.*, 2015). A highly negative correlation was found between $PM_{2.5}$ concentration and visibility, with a correlation coefficient of –0.77. It was also found that the mean concentration of $PM_{2.5}$ was as low as 18.6 μg m^{-3} during the 20%-best-visibility days, while it reached as high as 90.8 μg m^{-3} during the 20%-worst-visibility days. This prominent contrast highlighted the importance of $PM_{2.5}$ on visibility impairment (Li *et al.*, 2013). In addition, mixing layer height which determines the diffusion of air pollution in the vertical direction also had a great influence on $PM_{2.5}$, and a higher negative correlation coefficient of –0.66 was observed with $PM_{2.5}$ except for rainy days. Although a few days in phase 2 were rainy, the rainfall was relatively low. Some previous studies showed that the removal effect of

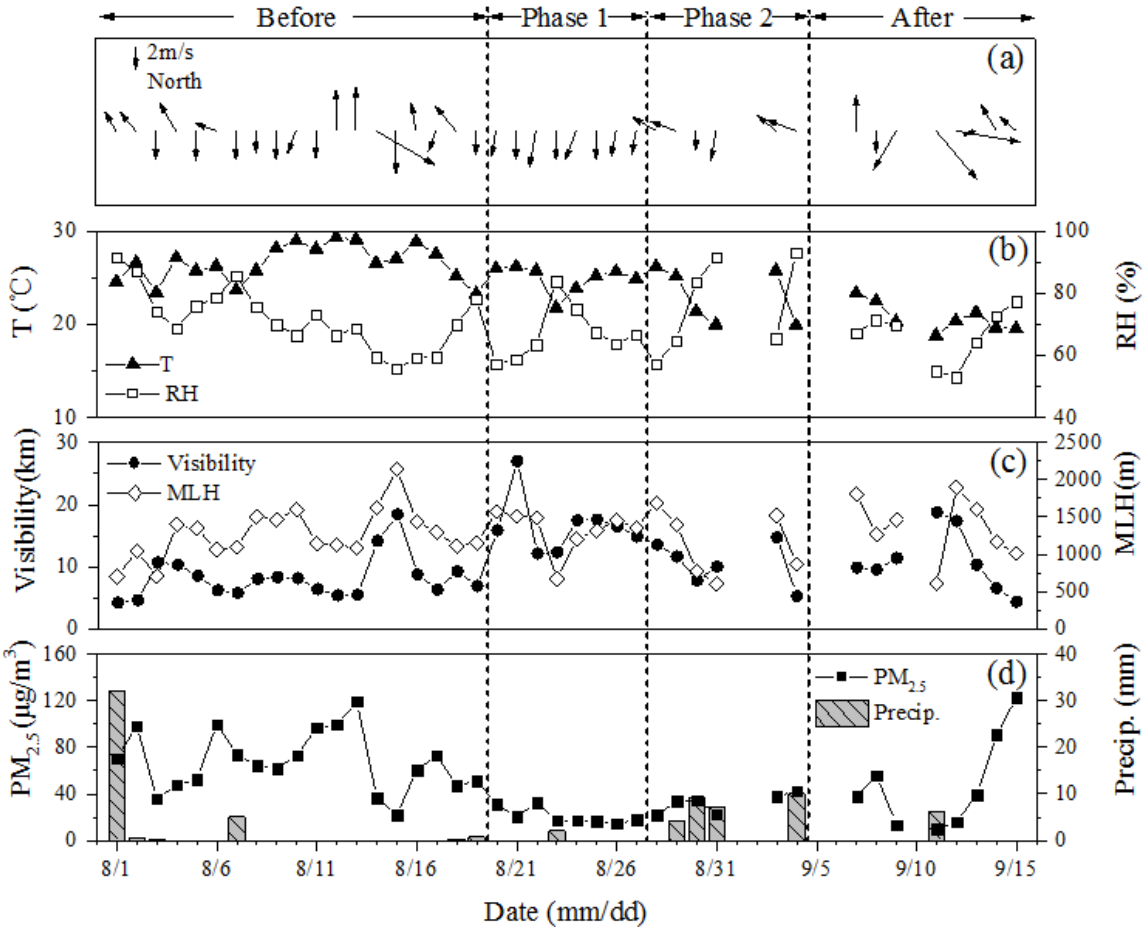

Fig. 2. Time series of (a) predominant wind direction and wind speed; (b) temperature (T) and relative humidity (RH); (c) visibility and mixing layer height (MLH) of daily maximum; and (d) $PM_{2.5}$ concentrations and precipitation.

light rain on $PM_{2.5}$ was not obvious, but the resulted low mixing layer height and high relative humidity during rainy days could promote the accumulation and generation of $PM_{2.5}$ (Wei *et al.*, 2015), and thus a relatively high $PM_{2.5}$ concentration was observed in phase 2 as shown in Fig. 2(d).

Table 2 presents the average concentration of $PM_{2.5}$ before, during and after the emission control measures (August 1 to 19; August 20 to 27; August 28 to September 4; September 5 to 15). During the emission control period, the concentration of $PM_{2.5}$ was reduced by 61.7%, comparing with no emission control period. This indicates that the stringent emission control played an important role on air quality improvement. It was noted that the average concentration of $PM_{2.5}$ increased by 53.8% in phase 2 as compared to phase 1 of the emission control period although a more rigorous emission reduction was implemented in phase 2. This unexpected $PM_{2.5}$ increase could be explained by the unfavorable meteorological condition, which was characterized by the occurrence of southerly wind (Fig. 2). According to cluster analysis results of 24 h air mass backward trajectories shown in Fig. 3 and the predominant wind direction shown in Fig. 2, nearly all of the air mass was from the north of Beijing in phase 1, but about 43% of the air mass in phase 2 was from southern Beijing. Previous study indicated that the anthropogenic emission was small in northern Beijing, while it was much higher in southern Beijing where many factories were located (Li *et al.*, 2014). This could lead to higher $PM_{2.5}$ concentration in phase 2 when southerly wind occurred. Moreover, during phase 2, the observed average $PM_{2.5}$ concentration in Baoding and Tianjin (e.g., south of Beijing) where trajectory 2, 3, and 4 (Fig. 3(b)) passing through was 43.2 and 33.8 μg m^{-3}, respectively, while the average $PM_{2.5}$ concentration in Chengde (e.g., north of Beijing) where trajectory 1 and trajectory 5 passing through was 13.5 μg m^{-3} (CNEMC, 2015). Such relatively high $PM_{2.5}$ concentration in the regions south of Beijing may also contribute to the increased $PM_{2.5}$ concentration in phase 2. Furthermore, as shown in Fig. 3(b), the air mass from the south of Beijing passed near the ground surface, making more polluted air mass being carried to Beijing and thus leading to increased $PM_{2.5}$. The above analysis illustrated that, to a certain extent, the transport of pollutants and meteorological conditions had a more prominent impact on $PM_{2.5}$ than emission reduction.

Table 2. Summary of mass concentrations of $PM_{2.5}$ and average meteorological parameters at different periods.

	Before	During			After
		Phase 1	Phase 2	Entire	
$PM_{2.5}$ (μg m^{-3})	67.6	21.0	32.3	25.9	48.3
Wind speed (m s^{-1})	2.3	2.4	2.4	2.4	2.8
T (°C)	26.6	24.9	23.1	24.1	20.7
RH (%)	71.7	67.0	75.9	70.8	66.3
MLH (m)	1264.9	1322.5	1141.8	1245.1	1352.5

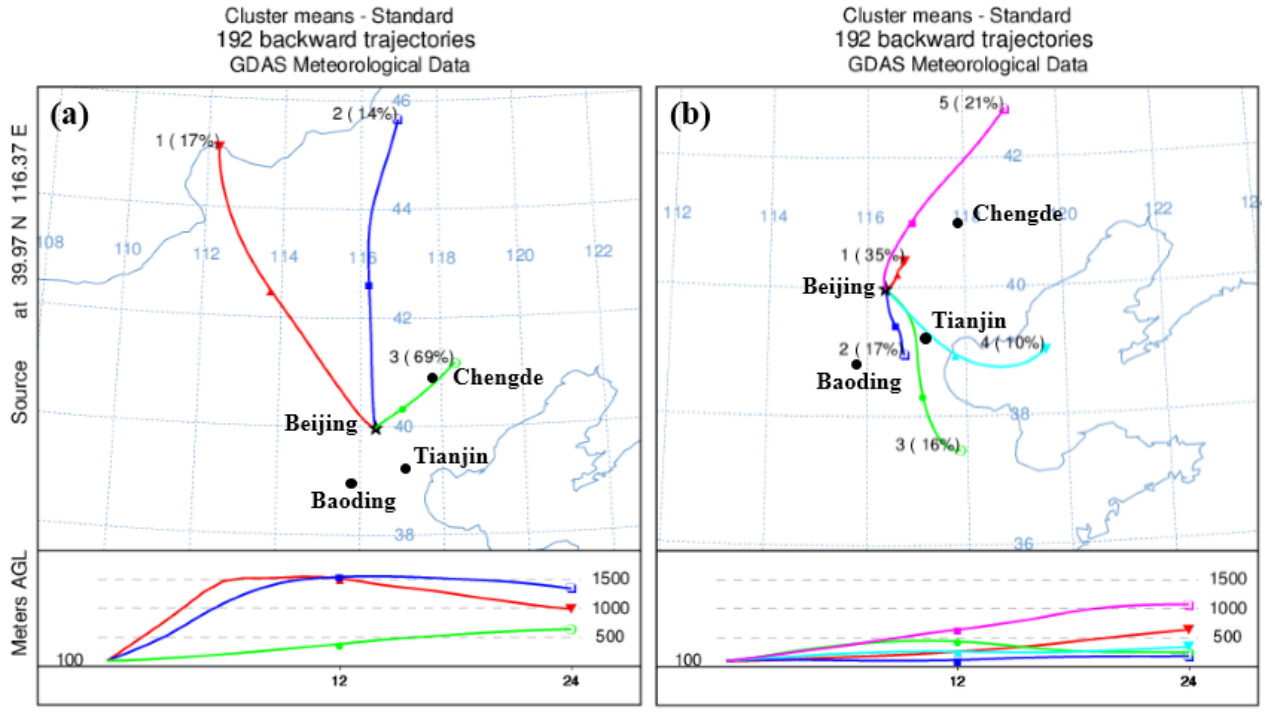

Fig. 3. Cluster analysis results of 24 h air mass backward trajectories during phase 1 (a) and phase 2 of emission reduction (b).

Ionic Components of $PM_{2.5}$

Table 3 presents the monitoring results of water-soluble ions in $PM_{2.5}$ during the study period. In this study, the secondary water-soluble ions (SWSI) including SO_4^{2-}, NO_3^-, and NH_4^+ were found as the main ions present in $PM_{2.5}$, accounting for 73.3% of the total water-soluble ions during the entire study period although this proportion varied before, during and after the emission control period. Fig. 4 shows the time series of the mass concentrations of SO_4^{2-}, NO_3^-, NH_4^+, Ca^{2+}, Mg^{2+}, K^+, Na^+, and Cl^- during the study period. It was observed that SO_4^{2-}, NO_3^- and NH_4^+ correlated well with $PM_{2.5}$, and the correlation coefficient was 0.95, 0.94 and 0.98, respectively. The concentrations of these three ions were high on August 2, August 6, August 11 to 13, and September 14 to 15 but low during the emission reduction period, illustrating that these three ions had a great contribution to $PM_{2.5}$. Some studies have shown that Cl^- might be derived from coal combustion when the mass ratio of Cl^-/Na^+ was larger than 1.17 for sea water (Wang *et al.,* 2016). The ratios of Cl^-/Na^+ were 1.99 ± 0.98, 1.45 ± 0.65, and 3.16 ± 2.45 before, during, and after the emission control period, respectively. It indicated that the effect of coal combustion emission control was better. The concentration of Ca^{2+} and Mg^{2+} was dramatically

Table 3. Mass concentration of major components in $PM_{2.5}$ at different periods (μg m^{-3}).

Species	Before	During			After
		Phase 1	Phase 2	Entire	
Cl^-	0.36 ± 0.20	0.15 ± 0.17	0.30 ± 0.16	0.21 ± 0.17	0.43 ± 0.28
NO_3^-	9.15 ± 5.13	2.82 ± 2.10	4.50 ± 2.55	3.54 ± 2.37	5.85 ± 5.58
SO_4^{2-}	8.49 ± 5.51	1.66 ± 1.00	2.68 ± 1.34	2.10 ± 1.23	5.94 ± 7.31
Na^+	0.21 ± 0.11	0.13 ± 0.07	0.18 ± 0.06	0.15 ± 0.07	0.22 ± 0.16
K^+	0.35 ± 0.25	0.16 ± 0.12	0.18 ± 0.17	0.17 ± 0.14	0.31 ± 0.40
Ca^{2+}	2.63 ± 0.59	1.16 ± 0.96	1.23 ± 0.96	1.19 ± 0.92	2.48 ± 1.39
Mg^{2+}	0.50 ± 0.49	0.09 ± 0.09	0.14 ± 0.10	0.11 ± 0.10	0.53 ± 0.62
NH_4^+	6.96 ± 3.57	1.70 ± 0.77	3.04 ± 1.24	2.28 ± 1.17	4.81 ± 4.82
Other ions	0.02 ± 0.01	0.01 ± 0.01	0.01 ± 0.01	0.01 ± 0.01	0.01 ± 0.01
S	3.60 ± 2.29	0.49 ± 0.38	1.35 ± 0.96	0.86 ± 0.79	2.70 ± 1.60
Na	1.10 ± 0.36	0.55 ± 0.38	0.57 ± 0.48	0.56 ± 0.40	0.69 ± 0.15
Mg	0.34 ± 0.24	0.18 ± 0.05	0.18 ± 0.11	0.18 ± 0.07	0.31 ± 0.45
Al	0.50 ± 0.44	0.14 ± 0.03	0.09 ± 0.08	0.13 ± 0.05	0.36 ± 0.11
Ca	1.41 ± 0.86	0.18 ± 0.12	0.58 ± 0.62	0.38 ± 0.47	0.94 ± 0.75
Ti	0.07 ± 0.06	0.05 ± 0.04	0.05 ± 0.06	0.05 ± 0.05	0.07 ± 0.03
Cr	0.03 ± 0.01	0.02 ± 0.01	0.02 ± 0.02	0.02 ± 0.02	0.02 ± 0.02
Fe	0.77 ± 0.27	0.40 ± 0.15	0.53 ± 0.27	0.45 ± 0.19	0.63 ± 0.44
Cu	0.03 ± 0.02	0.01 ± 0.01	0.02 ± 0.01	0.01 ± 0.01	0.03 ± 0.03
Zn	0.10 ± 0.12	0.02 ± 0.06	0.01 ± 0.01	0.01 ± 0.04	0.13 ± 0.30
Pb	0.06 ± 0.02	0.02 ± 0.01	0.03 ± 0.01	0.02 ± 0.01	0.06 ± 0.03
Other elements	0.02 ± 0.01	0.01 ± 0.01	0.01 ± 0.01	0.01 ± 0.01	0.02 ± 0.02
OC	10.34 ± 4.46	4.17 ± 2.14	5.76 ± 1.02	4.85 ± 1.88	7.02 ± 5.52
EC	3.61 ± 1.82	1.31 ± 0.54	1.80 ± 0.49	1.52 ± 0.56	2.64 ± 1.94

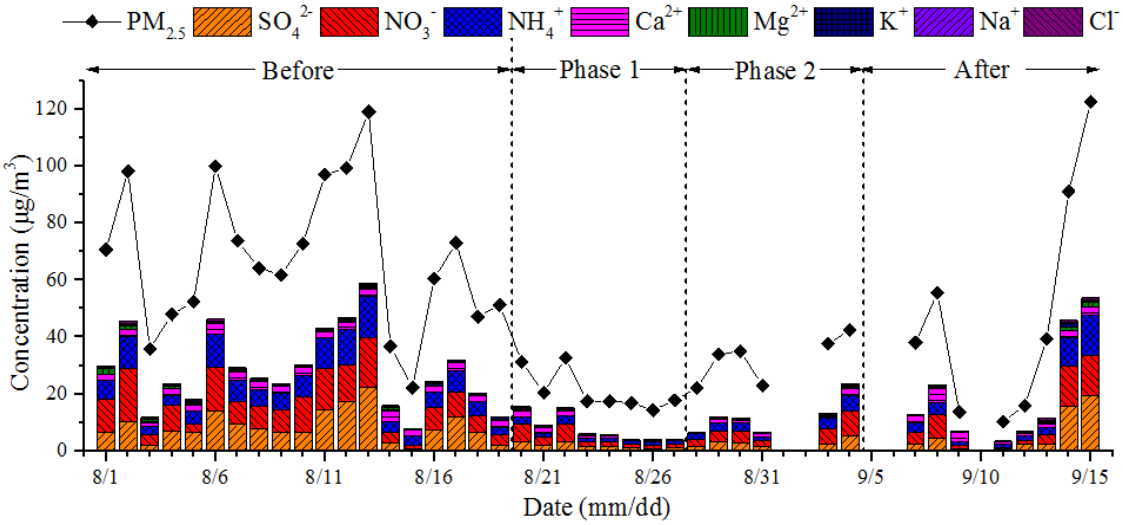

Fig. 4. Time series of the mass concentrations of $PM_{2.5}$, SO_4^{2-}, NO_3^-, NH_4^+, Ca^{2+}, Mg^{2+}, K^+, Na^+ and Cl^-.

decreased during the emission control period and rapidly increased after emission reduction. This indicated that the measures of stopping construction and strengthening of road sweeping had a significant impact on the concentration of $PM_{2.5}$ because the main sources of Ca^{2+} and Mg^{2+} were soil dust, road dust and construction dust. K^+ mainly came from biomass burning (Zhang *et al.*, 2013). Because of summertime and the emission control during the study period, the concentration of K^+ was at a low level.

The total water-soluble ions (TWSI) of $PM_{2.5}$ accounted for 41.5 ± 4.3%, 35.5 ± 10.0%, and 41.0 ± 6.3% of the total mass of $PM_{2.5}$ before, during, and after the emission control period, respectively. The proportion of the TWSI in $PM_{2.5}$ decreased significantly during the emission control period. During the entire emission control period, the average concentration of SWSI (SO_4^{2-}, NO_3^-, and NH_4^+) was decreased by 75.3%, 61.3%, and 67.3%, respectively, comparing with the period before emission control. The drop of SO_4^{2-} concentration was the largest because SO_4^{2-} was mainly converted from its precursor SO_2 which was a major gaseous pollutant. The regional cooperative emission control has ensured a significantly decreased SO_2 emission. However, a least decrease in the concentration of NO_3^- was observed. This was because the NO_3^- was mostly converted from its precursor NO_x which was mainly from vehicle emissions. Although the NO_x emission was reduced because of the traffic control measures, the absolute amount of vehicles running in Beijing was still remained at a high level. The drop of NH_4^+ concentration was slightly less than that of SO_4^{2-}. The NH_4^+ was mainly resulted from the reaction between NH_3 and the acid components of NO_3^- and SO_4^{2-} (He *et al.*, 2011). The NH_3 emission was mainly from human activities and natural sources, and the cooperative emission control measures led to reduced NH_3 emission. Consequently, a decreased NH_4^+ concentration could be resulted due to the reduced NH_3 emission and the decreased NO_3^- and SO_4^{2-} in the atmosphere (Rumsey *et al.*, 2011).

Comparing the concentrations of the main ions in $PM_{2.5}$ during phase 1 with those during phase 2, SO_4^{2-}, NO_3^-, and NH_4^+ increased by 1.02, 1.67 and 1.33 μg m^{-3}, respectively. According to the above analysis, a significant portion of air mass during phase 2 was from the south of Beijing, which had large emissions of SO_2 and NO_x, the precursors of secondary inorganic particles. Because of the regional transport of pollutants and the higher humidity, the concentrations of SO_4^{2-}, NO_3^-, and NH_4^+ during phase 2 were much higher than those during phase 1.

The equivalent charge ratio of the major cations Na^+, NH_4^+, K^+, Mg^{2+}, and Ca^{2+} to major anions SO_4^{2-}, NO_3^-, and Cl^- was used to indicate the neutralizing level of $PM_{2.5}$. The cation equivalent (CE) = $Na^+ + NH_4^+ + K^+ + Mg^{2+} + Ca^{2+}$, and the anion equivalent (AE) = $SO_4^{2-} + NO_3^- + Cl^-$. In this equation, CE/AE ≥ 1 indicated that most of the acids could be neutralized, while CE/AE < 1 indicated the aerosol was acidic (He *et al.*, 2011). Fig. 5 shows the correlations between CE and AE before and during the emission control period. The slope of the linear regression was 0.96 with a correlation coefficient R^2 = 0.98 before emission control period, indicating that the aerosol was acidic. And the slope of the linear regression was 1.03 with a correlation coefficient R^2 = 0.98 during emission control period, indicating that the anions were fully neutralized by cations. The comparisons between the two periods showed that the proportion of acidity in the atmosphere reduced during the emission control period, which indicated the effect of SO_2 and NO_x emission control was significant.

The mass ratio of NO_3^-/SO_4^{2-} had been used as an indicator of the relative importance of stationary versus mobile sources of sulfur and nitrogen in the atmosphere (Yao *et al.*, 2002). Typical mass ratio of NO_x and SO_x was reported as 8:1 to 13:1 from gasoline and diesel combustion emissions and 1:2 from coal combustion emissions, respectively (Chen *et al.*, 2015). Therefore, the higher ratio of NO_3^-/SO_4^{2-}, the more contribution of mobile sources than stationary sources to $PM_{2.5}$. The emission control of stationary sources was usually better in developed countries,

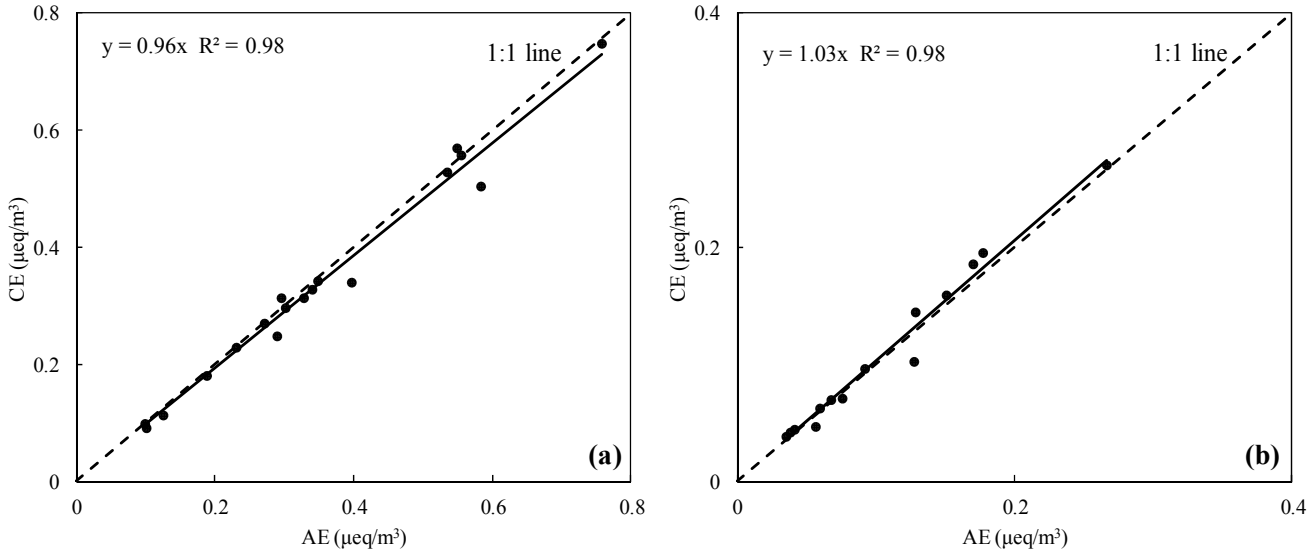

Fig. 5. Correlations between cations and anions before (a) and during (b) emission control period.

so their mobile sources had a greater contribution to $PM_{2.5}$ with a higher ratio of NO_3^-/SO_4^{2-}. For example, the ratio of NO_3^-/SO_4^{2-} in $PM_{2.5}$ in Los Angeles was reported as 2 (Kim *et al.*, 2000). However, in most areas of China, stationary source of emission from coal burning was still the main source of atmospheric pollutants, and the ratio of NO_3^-/SO_4^{2-} in $PM_{2.5}$ was normally about 0.3 to 0.5 (Xu *et al.*, 2012; Tao *et al.*, 2013). The ratio of NO_3^-/SO_4^{2-} was 1.7 ± 0.4 during the emission control period, which was higher than that before (1.2 ± 0.4) and after (1.2 ± 0.5) emission control. Meanwhile, as shown in Fig. 4, the concentration of NO_3^- was higher than that of SO_4^{2-} during the entire emission control period. This implies that the emission reductions during the study period from stationary sources were more than those from mobile sources. As a result, after taking a series of emission control measures, the $PM_{2.5}$ pollution from mobile source was more outstanding.

Inorganic Element in $PM_{2.5}$

The mean concentrations of 23 elements during entire periods were given in Table 3. The percentages of total detected elements accounted for 12.2 ± 2.5%, 10.7 ± 3.4%, and 13.5 ± 3.0% of $PM_{2.5}$ before, during, and after the emission control period, respectively. S was one of the major elemental components in $PM_{2.5}$, its origin is mainly anthropogenic being produced by burning of fossil fuels, in vehicle, and power production (Cohen *et al.*, 2004). The concentration of S was dramatically decreased during the emission control period, which indicated that the measures of strict supervision of anthropogenic sources had a significant impact on $PM_{2.5}$. The crustal elements (i.e., Na, Mg, Al, Ca, and Fe) were mainly from soil or construction dust. The concentration of this five elements was decreased by 39.9% to 76.6%. It indicated that the measures of stopping construction and strengthening of road sweeping had a significant impact on the concentration of $PM_{2.5}$.

Cu was used as an indicator for wear debris of vehicle (Lin *et al.*, 2014). Pb is coal combustion's tracer. The variation of Cu/Pb during entire study periods can be indicated that the relative importance of mobile versus stationary sources. The ratio of Cu/Pb was 0.42 ± 0.38, 0.54 ± 0.20, and 0.41 ± 0.27 before, during, and after the emission control period, respectively. The ratio variation agreed with NO_3^-/SO_4^{2-}, which further explained that the $PM_{2.5}$ pollution from mobile sources was relatively outstanding during the emission control period.

Carbonaceous Species of $PM_{2.5}$

Carbonaceous species represent a significant fraction of $PM_{2.5}$ in Beijing. In this study, carbonaceous species were divided into two major subtypes: organic carbon (OC) and elemental carbon (EC). It was found that OC and EC accounted for 16.8 ± 4.6% and 5.8 ± 1.6% of $PM_{2.5}$ during the entire study period. The mean concentrations of OC and EC during four periods were given in Table 3. During the entire emission control period, OC and EC mass concentrations were decreased by 53.1% and 57.9%, respectively, as compared with those before the emission control.

The relationship between OC and EC was very useful in assessing the origin of carbonaceous particles. A strong correlation between OC and EC indicates that they were predominantly emitted from a single source (Park *et al.*, 2001). Fig. 6 presents the correlation between OC and EC before and during the emission control period. A relatively strong correlation was found between OC and EC both before (R^2 = 0.73) and during (R^2 = 0.82) the emission control. This indicates that the OC and EC constituents may come from one single emission source, probably vehicle emissions, as both OC and EC were emitted significantly from internal combustion engines, especially diesel vehicles. Several investigators used OC/EC ratios to identify the sources of carbonaceous species (Ram *et al.*, 2008). Some studies reported OC/EC ratios of 1.0 to 4.2 for traffic emissions and 2.5 to 10.5 for coal combustion emissions, while OC/EC ratio greater than 2 had been used for the identification and evaluation of secondary organic carbon (SOC) (Chen *et al.*, 2006). In this study, the mass ratio of OC/EC before and during emission control was 3.0 ± 0.6 and 3.2 ± 0.4, respectively. Using EC tracer method (Castro *et al.*, 1999), the SOC concentrations before and during emission control were determined as 2.6 ± 2.3 and 1.6 ±

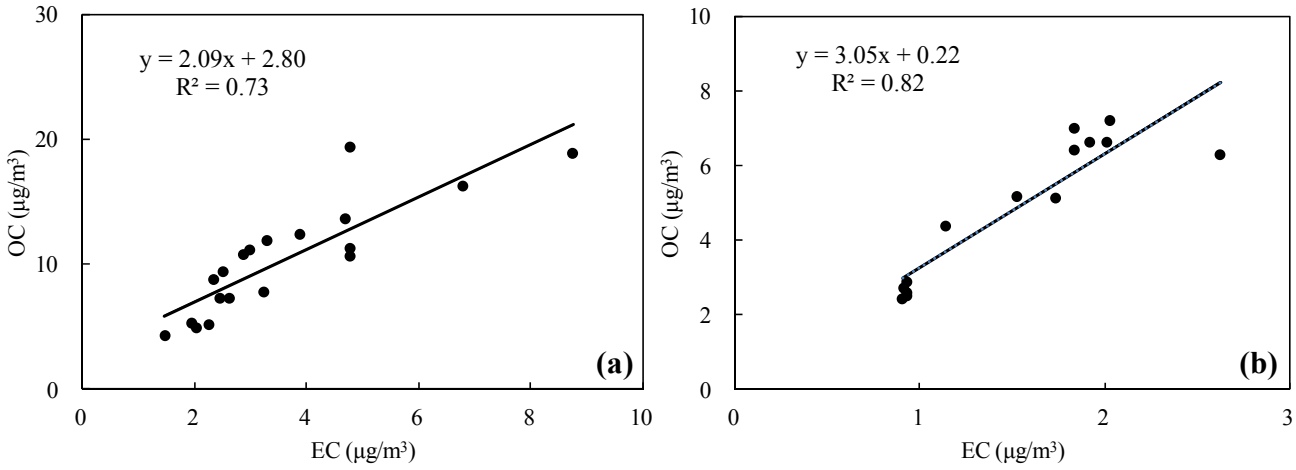

Fig. 6. Correlation between OC and EC concentrations before (a) and during (b) emission control period.

0.9 μg m^{-3}, accounting for 24.0 ± 15.7% and 30.7 ± 10.0% of the total mass of OC, respectively. Compared the SOC/OC ratios from this work and other research, the value were 56.5% (Xu *et al.*, 2015) and 50.2% (Yao *et al.*, 2016), which was higher than this study period. It indicated that SOC for the carbon component contribution was not obvious, and the main source of carbonaceous aerosols was vehicular emissions and coal combustion sources.

$PM_{2.5}$ Mass Balance

In this study, $PM_{2.5}$ mass balance was calculated (Fig. 7). The mass balance was classified into primary components and secondary components. The primary components include primary organic aerosol (POA), EC, soil dust, and pollution elements (S, V, Cr, Mn, Ni, Cu, Zn, As, Sr, Cd, Sb, and Pb). The secondary components include secondary organic aerosol (SOA), SO_4^{2-}, NO_3^-, and NH_4^+. The mass of SOA and POA could be converted from SOC and primary organic carbon (POC) by multiplying a coefficient of 1.6 (Chow *et al.*, 1996). Soil dust concentrations were calculated by the concentrations of the elements of Al, Ca, Fe, and Ti according to Eq. (1). In this study, Si was not measured and its concentration was estimated to be four times of Al (Wen *et al.*, 2016).

$$\text{Soil Dust} = 2.20 \times \text{Al} + 2.49 \times \text{Si} + 1.63 \times \text{Ca} + 2.42 \times \text{Fe} + 1.94 \times \text{Ti} \quad (1)$$

As shown in Fig. 7, the decrease of SO_4^{2-} percentage was the largest among all the SWSI ions, with SO_4^{2-} accounting for 15.2%, 9.6%, 10.3%, and 15.1% of the $PM_{2.5}$, respectively, during the four study periods. This indicates that the strict emission control in industrial enterprises had a significant impact on $PM_{2.5}$ concentration. The percentage of NO_3^- during the four periods was 16.1%, 16.3%, 16.3%, and 14.8%, respectively, with a little difference observed after emission control, and this is consistent with the results of ion analysis. In addition, Fig. 7 shows a clear increase in SOA on August 20, when emission control was firstly implemented in Beijing. During the entire emission control period, the organic matter (POA + SOA) accounted for 37.6% of the $PM_{2.5}$ mass, while this proportion was only 29.3% and 28.5% before and after the emission control. The soil dust accounted for 12.1%, 10.2%, 10.9%, and 12.6% of the total mass of $PM_{2.5}$, respectively, during four study periods. The percentage of soil dust mass in $PM_{2.5}$ during emission control period decreased considerably, indicating that the measures of stopping construction and strengthening of road sweeping were effective. The variation trend of pollution elements was the same as that of soil dust. In addition, the percentage of soil dust, pollution elements, and SWSI in $PM_{2.5}$ during phase 2 was slightly higher than that during phase 1.

CONCLUSIONS

A large-scale parade was held in Beijing on September 3, 2015 to commemorate the 70th anniversary of the victory of the Chinese People's Anti-Japanese War and the World Anti-fascist War. A phased emission control measures were taken in Beijing and its surrounding provinces in order to improve the air quality during the parade. Such large-scale open experiments provided an excellent opportunity of investigating the pollution characteristics in Beijing. In this study, $PM_{2.5}$ samples were collected in Beijing before, during, and after the emission control for this international parade event. The observed $PM_{2.5}$ and meteorological data as well as the emission reduction measures were systematically analyzed. Air mass trajectory analysis based on HYSPLIT model was also used to examine the impact of pollutant regional transport on the pollution characteristics in Beijing. It was found that the concentration of $PM_{2.5}$ decreased significantly during the emission control period, but the concentration during phase 2 of emission control increased by 32.6% as compared to that during phase 1 due to the impact of regional pollutant transport and meteorological

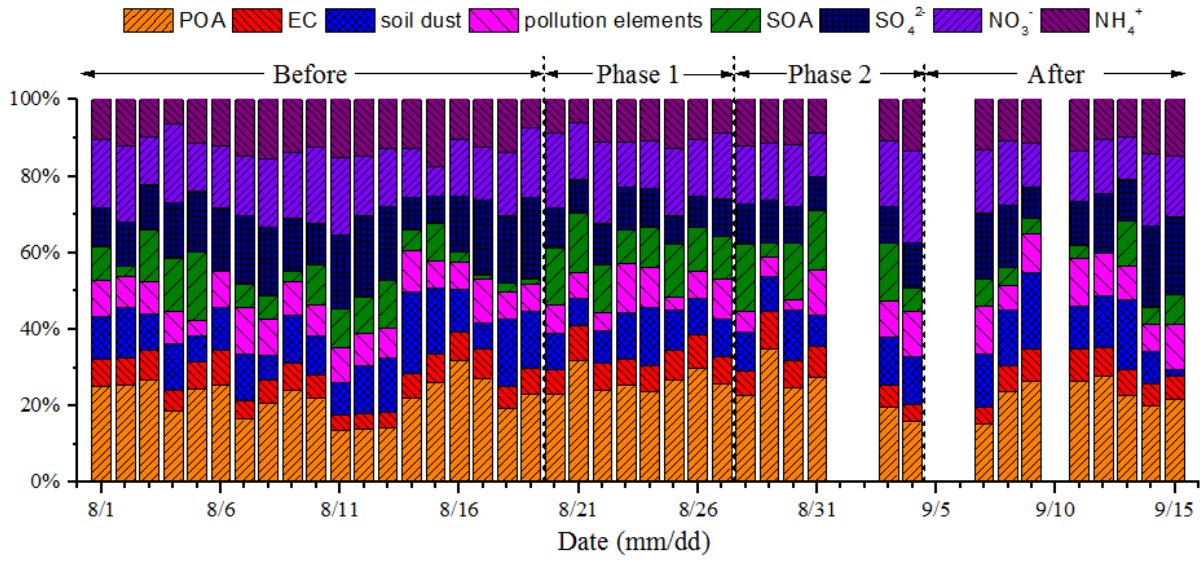

Fig. 7. Chemical compositions in mass percentage for the $PM_{2.5}$.

conditions. The secondary water-soluble ions including SO_4^{2-}, NO_3^-, and NH_4^+ were found as the main ions present in $PM_{2.5}$ in Beijing. During the emission control period, the drop of the concentration of Ca^{2+}, Mg^{2+}, and SO_4^{2-} was the largest comparing with other ions. The results also indicated that the measures of stopping construction, strengthening of road sweeping, and strict supervision of industrial enterprises had a significant impact on $PM_{2.5}$. The correlation between OC and EC concentrations and the OC/EC ratio showed that the main source of carbonaceous aerosols was vehicular emissions and coal combustion sources. Moreover, the ratio of NO_3^-/SO_4^{2-} and Cu/Pb during the emission control period was higher than before and after the emission control. It was shown that after taking a series of emission control measures, the contribution of mobile sources to $PM_{2.5}$ in Beijing was relatively outstanding.

ACKNOWLEDGMENTS

This work was supported by the National Natural Science Foundation of China (No. 91544232 & 51638001), National Key Technology Research and Development Program of the Ministry of Science and Technology of China (No. 2013BAC17B01 & 2014BAC23B00) and the Ministry of Environmental Protection Special Funds for Scientific Research on Public Causes (No. 201409006 & 201409003 & 201409007). In addition, we greatly appreciated the fund support from Beijing Municipal Commission of Science and Technology (No. Z141100001014002 & D16110900440000). The authors are grateful to the anonymous reviewers for their insightful comments.

REFERENCES

BMBS (Beijing Municipal Bureau of Statistics, China) (2015). http://www.bjstats.gov.cn/nj/main/2015-tjnj/zk/indexch.htm. Last Access: 5 February 2016 (in Chinese).

BMEPB (Beijing Municipal Environmental Protection Bureau, China) (2015). http://www.bjepb.gov.cn/bjepb/413526/331443/331937/333896/4376820/index.html Last Access: 5 February 2016 (in Chinese).

Castro, L.M., Pio, C.A., Harrison, R.M. and Smith, D.J.T. (1999). Carbonaceous aerosol in urban and rural European atmosphere: Estimation of secondary organic carbon concentrations. *Atmos. Environ*. 33: 2771–2781.

Chen, C., Sun, Y.L., Xu, W.Q., Du, W., Zhou, L.B., Han, T.T., Wang, Q.Q., Fu, P.Q., Wang, Z.F., Gao, Z.Q., Zhang, Q. and Worsnop, D.R. (2015). Characteristics and sources of submicron aerosols above the urban canopy (260 m) in Beijing, China, during the 2014 APEC summit. *Atmos. Chem. Phys*. 15: 12879–12895.

Chen, Y., Zhi, G., Feng, Y., Fu, J., Feng, J., Sheng, G. and Simoneit, B.R.T. (2006). Measurements of emission factors for primary carbonaceous particles from residential raw-coal combustion in China. *Geophys. Res. Lett*. 332: 382–385.

Cheng, S.Y., Jin, Y.Q., Liu, L., Huang, G.H., Hao, R.X. and Jansson, C.R. (2002). Estimation of atmospheric mixing heights over large areas using data from airport meteorological stations. *J. Environ. Sci. Health. Part A* 37: 991–1007.

Chow, J.C., Watson, J.G., Lu, Z., Lowenthal, D.H., Frazier, C.A., Solomon, P.A., Thuillier, R.H. and Magliano, K. (1996). Descriptive analysis of $PM_{2.5}$ and PM_{10} at regionally representative locations during SJVAQS/AUSPEX. *Atmos. Environ*. 30: 2079–2112.

Chow, J.C., Watson, J.G., Chen, L.W.A., Arnott, W.P., Moosmüller, H. and Fung, K. (2004). Equivalence of elemental carbon by thermal/optical reflectance and transmittance with different temperature protocols. *Environ. Sci. Technol.* 38: 4414–4422.

CNEMC (China National Environmental Monitoring Centre, China) (2015). http://106.37.208.233:20035/, Last Access: 5 February 2016 (in Chinese).

Cohen, D.D., Garton, D. and Stelcer, E., (2004). Multielemental analysis and characterization of fine aerosols at several key ACE-Asia sites. *J. Geophys. Res.* 109: 19–12.

Draxler, R.R. and Hess, G. (1997). *Description of the HYSPLIT4 Modeling System*, Air Resources Laboratory, Silver Spring, Maryland.

Fann, N. and Risley, D. (2013). The public health context for $PM_{2.5}$ and ozone air quality trends. *Air Qual. Atmos. Health* 6: 1–11.

Fu, Q., Zhuang, G., Wang, J., Chang, X., Huang, K., Li, J., Hou, B., Lu, T. and Streets, D.G. (2008). Mechanism of formation of the heaviest pollution episode ever recorded in the Yangtze River Delta, China. *Atmos. Environ*. 42: 2023–2036.

Gao, X., Nie, W., Xue, L., Wang, T., Wang, X., Gao, R., Wang, W., Chao, Y., Gao, J., Ravi, K.P., Wang, J. and Zhang, Q. (2013). Highly time-resolved measurements of secondary ions in $PM_{2.5}$ during the 2008 Beijing Olympics: The impacts of control measures and regional transport. *Aerosol Air Qual. Res*. 13: 367–376.

He, K., Zhao, Q., Ma, Y., Duan, F., Yang, F., Shi, Z., Chen, G. (2011). Spatial and seasonal variability of $PM_{2.5}$ acidity at two Chinese megacities: Insights into the formation of secondary inorganic aerosols. *Atmos. Chem. Phys*. 11: 25557–25603.

Huang, W., Fan, H., Qiu, Y., Cheng, Z. and Qian, Y. (2015). Application of fault tree approach for the causation mechanism of urban haze in Beijing-Considering the risk events related with exhausts of coal combustion. *Sci. Total Environ*. 544: 1128–1135.

Ji, D., Li, L., Wang, Y., Zhang, J., Cheng, M., Sun, Y., Liu, Z., Wang, L., Tang, G., Hu, B., Chao, N., Wen, T. and Miao, H. (2014). The heaviest particulate air-pollution episodes occurred in northern China in January, 2013: Insights gained from observation. *Atmos. Environ*. 92: 546–556.

Kim, B.M., Teffera, S. and Zeldin, M.D. (2000). Characterization of $PM_{2.5}$ and PM_{10} in the south coast air basin of Southern California: Part 1--Spatial variations. *J. Air Waste Manage. Assoc.* 50: 2034–2044.

Li, X., He, K., Li, C., Yang, F., Zhao, Q., Ma, Y., Cheng, Y., Ouyang, W. and Chen, G. (2013). $PM_{2.5}$ mass, chemical composition, and light extinction before and

during the 2008 Beijing Olympics. *J. Geophys. Res.* 118: 12158–12167.

Li, L., Li, M., Huang, Z., Gao, W., Nian, H., Fu, Z., Gao, J., Chai, F. and Zhou, Z. (2014). Ambient particle characterization by single particle aerosol mass spectrometry in an urban area of Beijing. *Atmos. Environ*. 94: 323–331.

Li, J. and Han, Z. (2015). A modeling study of severe winter haze events in Beijing and its neighboring regions. *Atmos. Res*. 170: 87–97.

Li, Y.J., Lee, B.P., Su, L., Fung, J.C.H. and Chan, C.K. (2015). Seasonal characteristics of fine particulate matter (PM) based on high resolution time-of-flight aerosol mass spectrometric (HR-ToF-AMS) measurements at the HKUST Supersite in Hong Kong. *Atmos. Chem. Phys*. 14: 20259–20293.

Lin, Y.C., Tsai, C.J., Wu, Y.C., Zhang, R., Chi, K.H., Huang, Y.T., Lin, S.H. and Hsu, S.C. (2014). Characteristics of trace metals in traffic-derived particles in Hsuehshan Tunnel, Taiwan: Size distribution, fingerprinting metal ratio, and emission factor. *Atmos. Chem. Phys*. 14: 13963–14004.

Meng, R., Zhao, F., Sun, K., Zhang, R., Huang, C. and Yang, J. (2015). Analysis of the "APEC Blue" in Beijing using more than one decade of satellite observations: Lessons learned from radical emission control measures. *Remote Sens*. 7: 15224–15243.

Okuda, T., Matsuura, S., Yamaguchi, D., Umemura, T., Hanada, E., Orihara, H., Tanaka, S., He, K., Ma, Y., Cheng, Y., Liang, L. (2011). The Impact of the Pollution Control Measures for the 2008 Beijing Olympic Games on the Chemical Composition of Aerosols. *Atmos. Environ*. 45: 2789–2794.

Ouyang, W., Guo, B., Cai, G., Li, Q., Han, S., Liu, B. and Liu, X. (2015). The washing effect of precipitation on particulate matter and the pollution dynamics of rainwater in downtown Beijing. *Sci. Total Environ.* 505: 306–314.

Park, S.S., Kim, Y.J. and Fung, K. (2001). Characteristics of $PM_{2.5}$ carbonaceous aerosol in the Sihwa industrial area, Korea. *Atmos. Environ*. 35: 657–665.

Ram, K., Sarin, M.M. and Hegde, P. (2008). Atmospheric abundances of primary and secondary carbonaceous species at two high-altitude sites in India: Sources and temporal variability. *Atmos. Environ*. 42: 6785–6796.

Rumsey, I.C., Cowen, K.A., Walker, J.T., Kelly, T.J., Hanft, E.A., Mishoe, K., Rogers, C., Proost, R., Beachley, G.M., Lear, G., Frelink, T. and Otjes, R.P. (2011). An assessment of the performance of the Monitor for AeRosols and GAses in ambient air (MARGA): A semi-continuous method for soluble compounds. *Atmos. Chem. Phys*. 14: 5639–5658.

Schleicher, N., Norra, S., Chen, Y., Chai, F. and Wang, S. (2012). Efficiency of mitigation measures to reduce particulate air pollution—A case study during the Olympic Summer Games 2008 in Beijing, China. *Sci. Total Environ.* 427–428: 146–58.

Song, S., Wu, Y., Jiang, J., Yang, L., Cheng, Y. and Hao, J. (2012). Chemical characteristics of size-resolved $PM_{2.5}$ at a roadside environment in Beijing, China. *Environ. Pollut*. 161: 215–221.

Sun, Y., Qi, J., Wang, Z., Fu, P., Li, J., Yang, T. and Yin, Y. (2014). Investigation of the sources and evolution processes of severe haze pollution in Beijing in January 2013. *J. Geophys. Res.* 119: 4380–4398.

Tang, G., Zhu, X., Hu, B., Xin, J., Wang, L., Münkel, C., Mao, G. and Wang, Y. (2015). Impact of emission controls on air quality in Beijing during APEC 2014: Lidar ceilometer observations. *Atmos. Chem. Phys*. 15: 12667–12680.

Tao, J., Cheng, T., Zhang, R., Cao, J., Zhu, L., Wang, Q., Luo, L. and Zhang, L. (2013). Chemical Composition of $PM_{2.5}$ at an Urban Site of Chengdu in Southwestern China. *Adv. Atmos. Sci*. 30: 1070–1084.

Tao, M., Chen, L., Xiong, X., Zhang, M., Ma, P., Tao, J. and Wang, Z. (2014). Formation process of the widespread extreme haze pollution over northern China in January 2013: Implications for regional air quality and climate. *Atmos. Environ*. 98: 417–425.

Wang, H., Xu, J., Zhang, M., Yang, Y., Shen, X., Wang, Y., Chen, D. and Guo, J. (2014a). A study of the meteorological causes of a prolonged and severe haze episode in January 2013 over central-eastern China. *Atmos. Environ*. 98: 146–157.

Wang, L., Zhang, N., Liu, Z., Sun, Y., Ji, D. and Wang, Y. (2014b). The influence of climate factors, meteorological conditions, and boundary-layer structure on severe haze pollution in the Beijing-Tianjin-Hebei region during January 2013. *Adv. Meteorol.* 2014: 685971.

Wang, H., Tian, M., Li, X., Chang, Q., Cao, J., Yang, F., Ma, Y. and He, K. (2015). Chemical composition and light extinction contribution of $PM_{2.5}$ in urban Beijing for a 1-year period. *Aerosol Air Qual. Res.* 15: 2200–2211

Wang, Y., Zhuang, G. and Tang, A. (2005). The ion chemistry and the source of $PM_{2.5}$ aerosol in Beijing. *Atmos. Environ*. 39, 3771–3784.

Wen, W., Cheng, S., Chen, X., Wang, G., Li, S., Wang, X. and Liu, X. (2016). Impact of emission control on $PM_{2.5}$ and the chemical composition change in Beijng-Tianjin-Hebei during the APEC summit 2014. *Environ. Sci. Pollut. Res. Int.* 23: 4509–4521.

Xu, L., Chen, X., Chen, J., Zhang, F., He, C., Zhao, J. and Yin, L. (2012). Seasonal variations and chemical compositions of $PM_{2.5}$ aerosol in the urban area of Fuzhou, China. *Atmos. Res*. 104: 264–272.

Xu, W.Q., Sun, Y.L., Chen, C., Du, W., Han, T.T., Wang, Q.Q., Fu, P.Q., Wang, Z.F., Zhao, X.J., Zhou, L.B., Ji, D.S., Wang, P.C. and Worsnop, D.R. (2015). Aerosol composition, oxidative properties, and sources in Beijing: Results from the 2014 Asia-Pacific Economic Cooperation Summit study. *Atmos. Chem. Phys*. 15: 23407–23455.

Xu, Z., Wen, T., Li, X., Wang, J. and Wang, Y. (2015). Characteristics of carbonaceous aerosols in Beijing based on two–year observation. *Atmos. Pollut. Res*. 6: 202–208.

Yao, L., Yang, L., Chen, J., Wang, X., Xue, L., Li, W., Sui, X., Wen, L., Chi, J., Zhu, Y., Zhang, J., Xu, C., Zhu, T. and Wang, W. (2016). Characteristics of carbonaceous

aerosols: Impact of biomass burning and secondary formation in summertime in a rural area of the North China Plain. *Sci. Total Environ.* 557–558: 520–530.

Yao, X., Chan, C.K., Fang, M., Cadle, S., Chan, T., Mulawa, P., He, K and Ye, B. (2002). The water-soluble ionic composition of $PM_{2.5}$ in Shanghai and Beijing, China. *Atmos. Environ*. 36: 4223–4234.

Zhang, R., Jing, J., Tao, J., Hsu, S.C., Wang, G., Cao, J., Lee, C.S.L., Zhu, L., Chen, Z., Zhao, Y. and Shen, Z. (2013). Chemical characterization and source apportionment of $PM_{2.5}$ in Beijing: Seasonal perspective. *Atmos. Chem. Phys*. 13: 7053–7054.

Zhang, X.Y., Wang, J.Z, Wang, Y.Q., Liu, H.L., Sun, J.Y. and Zhang, Y.M. (2015). Changes in chemical components of aerosol particles in different haze regions in China from 2006 to 2013 and contribution of meteorological factors. *Atmos. Chem. Phys*. 15: 12935–12952.

Received for review, July 20, 2016
Revised, October 11, 2016
Accepted, November 10, 2016